Invited Paper

Context Recognition by Wireless Sensing: A Comprehensive Survey

Akira Uchiyama[1,2,a)] Shunsuke Saruwatari[1,b)] Takuya Maekawa[1,c)]
Kazuya Ohara[3,d)] Teruo Higashino[1,e)]

Received: September 10, 2020, Accepted: October 23, 2020

Abstract: Context recognition is a topic that has garnered considerable interest in the ubiquitous and pervasive computing research community. A wide variety of Internet-of-things devices with micro-electromechanical system (MEMS) sensors are used to obtain sensor data (e.g., acceleration, vibration, and sound) related to target contexts. However, devices for context recognition also have limitations such as deployment cost, battery maintenance cost, and the requirement for wearing/carrying the devices. To solve this problem, wireless sensing has attracted the attention of many researchers because it enables device-free and/or maintenance-free context recognition. In this study, we will comprehensively review studies on context recognition by wireless sensing, focusing on WiFi channel state information (CSI), radio-frequency identification (RFID), and backscatter. We will also discuss the design choices of wireless sensing with their pros and cons through a review of the state-of-the-art.

Keywords: context recognition, channel state information, wireless sensing, backscatter

1. Introduction

Wireless technologies have become indispensable to our daily lives. We are surrounded by various radio frequency (RF) signals such as TV, FM/AM radio, cellular signals, WiFi, and Bluetooth. They are used for data transmission. However, recent research efforts have discovered a new aspect of wireless technologies—*wireless sensing*. Wireless sensing enables us to recognize various contexts by leveraging RF signals change due to contexts such as human motions and object movements. Typical wireless sensing methods involve transmitters (Tx) for lighting up targets and receivers (Rx) for capturing RF change due to context. WiFi base stations, laptops, smartphones, and RFID (radio frequency identification) readers are often used as Tx and Rx. This means that Tx and Rx in wireless sensing have plenty of energy resources, such as large batteries and power outlets, compared with small Internet-of-things (IoT) devices such as wearables. In this sense, wireless sensing is one of the key enablers for context sensing without the maintenance of batteries.

This paper comprehensively reviews studies on context recognition by wireless sensing, focusing on WiFi CSI (channel state information), RFID, and backscatter. **Figure 1** illustrates the overview of wireless sensing by WiFi CSI, RFID, and backscatter. The original purpose of WiFi CSI is multiple-input and multiple-output (MIMO) communication to estimate the states of signal propagation paths. Intuitively, WiFi CSI represents physical movements due to contexts because physical movements incur state changes in signal propagation paths. RFID has also attracted the attention of many researchers because RFID readers can directly recognize the precise movement of RFID tags attached to targets. The other key feature of RFID tags is battery-free operation, as it is powered by the RF signal from an RFID reader. By observing RF signals reflected from RFID tags, the RFID reader can recognize the movement of RFID tags. Lastly, backscatter is a technique for ultra-low power wireless communication wherein communication is enabled by reflecting the carrier waves emitted from external RF signal sources. Its basic principle is widely used for low-power communication of RFID systems. In Ref. [1], a novel concept of ambient backscatter was first proposed, which leverages ambient RF signals such as TV as an external RF signal source for backscatter communication. The original purpose of backscatter is data transmission, similar to other wireless technologies. However, recent studies have revealed the feasibility of wireless sensing by directly converting physical motions and phenomena (contexts) into changes in RF signals.

Many survey papers have already been published on wireless sensing by WiFi CSI [2], [3], [4], [5]. In this study, we leave a detailed review of wireless sensing by WiFi CSI to these survey papers. Instead, we focus on reviewing the differences between WiFi CSI, RFID, and backscatter along with the state-of-the-art in each stream.

The main challenge to exploit WiFi CSI is noise mitigation. WiFi CSI suffers from noise due to clock offsets between Tx and Rx (carrier frequency offsets (CFO), sampling frequency offsets

[1] Graduate School of Information Science and Technology, Osaka University, Suita, Osaka 565–0871, Japan
[2] JST, PRESTO
[3] NTT Communication Science Laboratories, “Keihanna Science City”, Kyoto 619–0237, Japan
[a)] uchiyama@ist.osaka-u.ac.jp
[b)] saru@ist.osaka-u.ac.jp
[c)] maekawa@ist.osaka-u.ac.jp
[d)] kazuya.ohara.hm@hco.ntt.co.jp
[e)] higashino@ist.osaka-u.ac.jp

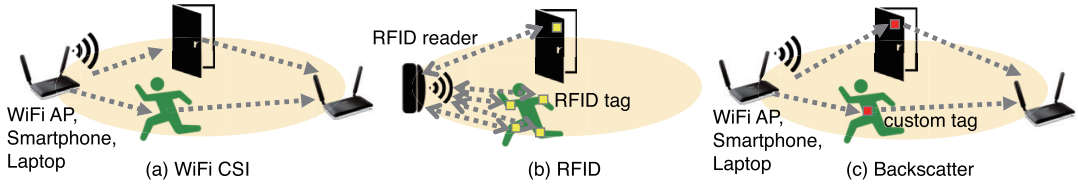

Fig. 1 Wireless sensing overview.

(SFO), and packet detection delay (PDD)). Many studies have employed sophisticated methods to mitigate such noises. Some methods apply additional processing to alleviate multipath effects. After CSI preprocessing, context recognition is performed by signal propagation models or machine learning-based models such as deep learning.

By contrast, RFID systems do not have clock offsets because the RFID reader serves as both Tx and Rx. Instead, the effects of multipath antenna orientation, and hardware imperfection are the major sources of noise. Research efforts have been made to deal with such effects. Because RFID phase information is more reliable than the CSI phase, many approaches are based on basic physics, which include the relation between wavelength, distance, and phase. In this sense, wireless sensing by RFID is more accurate and precise than WiFi-based wireless sensing. Another advantage of RFID tags is their inherent ability to identify targets (i.e., attached parts, subjects, or objects) by responding to their presence with their identification.

Wireless sensing by backscatter is an emerging *new classical* technique. Unlike other wireless sensing approaches, wireless sensing by backscatter *directly* converts contexts (e.g., temperature, pressure, moisture, and audio) into changes in the backscattered wireless signal. Backscatter communication is an ultra-low power and promising building block for future IoTs. Nevertheless, it still requires digital modulation, which necessitates processing by computation modules such as microcontroller units. This leads to additional costs for additional components as well as additional energy consumption, which can limit the application design space. Wireless sensing by backscatter leverages analog sensors or physical movements due to contexts (e.g., wind, water flow, and acoustic vibration). Its design is simple, yet worth exploring with the application space, opening up new vistas of wireless sensing.

The remainder of this paper is as follows. Section 2 describes the basic principle of WiFi CSI, followed by a review of the state-of-the-art. Section 3 presents a review of RFID sensing with an overview of RFID systems. Section 4 describes a review of wireless sensing by backscatter. In Section 5, we describe the design choices of wireless sensing through a discussion on the pros and cons of WiFi CSI, RFID, and backscatter. Finally, Section 6 concludes the paper.

2. Channel State Information

2.1 Basic Principle of WiFi CSI

In wireless LAN standards IEEE 802.11n and later, MIMO is adopted to improve the quality of communication. In addition, orthogonal frequency-division multiplexing (OFDM) is used as a modulation scheme that uses multiple orthogonal subcarriers. MIMO leverages CSI for transmission signal control to improve the quality of the signal at the receiver side. CSI provides the amplitude and phase differences for each subcarrier in this OFDM modulation. Let $\boldsymbol{X}(f,t)$ and $\boldsymbol{Y}(f,t)$ be the frequency domain representations of the transmitted and received signals, respectively, with carrier frequency f at time t. The relationship between $\boldsymbol{X}(f,t)$ and $\boldsymbol{Y}(f,t)$ are written as

$$\boldsymbol{Y}(f,t) = \boldsymbol{H}(f,t) \cdot \boldsymbol{X}(f,t), \tag{1}$$

where $\boldsymbol{H}(f,t)$ is the complex-valued channel frequency response (CFR).

Assuming that the number of subcarriers is S for N_{T_x} antennas of the transmitter and N_{R_x} antennas of the receiver, we can obtain $N_{T_x} \cdot N_{R_x} \cdot S$ pairs of CFR values, which is called CSI. Using commercial WiFi devices such as Intel 5300 NIC with a modified driver, we can obtain CSI samples. Compared to RSSI, CSI contains richer information on the conditions of the radio propagation paths. Because the channel states change due to dynamic components such as human movement, CSI has been used to improve communication quality and context recognition.

As the signal travels from a transmitter to a receiver through multiple paths including the direct path, reflection from walls, and human bodies, CSI is the superposition of components from all the paths as follows.

$$\boldsymbol{H}(f,t) = e^{-j2\pi ft} \sum_{\forall p} a_p(f,t)\, e^{-j2\pi f d_p(t)/c}, \tag{2}$$

where $a_p(f,t)$ and $d_p(t)$ are the amplitude attenuation factor and the length of the p-th path at time t, respectively. c is the speed of light.

To extract signals due to object/human movements, many approaches model the CSI as a composition of static and dynamic components as follows.

$$\boldsymbol{H}(f,t) = \boldsymbol{H}_d(f,t) + \boldsymbol{H}_s(f,t), \tag{3}$$

where $\boldsymbol{H}_d(f,t)$ and $\boldsymbol{H}_d(f,t)$ are the CSI of the dynamic and static components, respectively.

2.2 CSI Noise Factors

CSI is estimated by sending pilot signals from a transmitter to a receiver. In practice, the estimated CSI is distorted by various noise factors owing to hardware imperfection. The following factors have been mentioned in many existing works [6], [7], [8], [9], [10].

- **CFO:** CFO is introduced because the oscillators of the transmitter and the receiver are not exactly synchronized. This means that there is an offset between the central frequencies

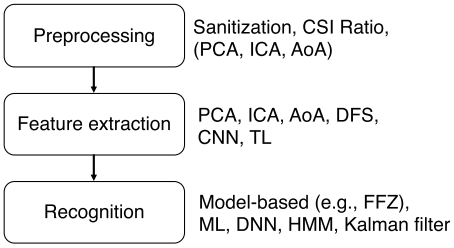

Fig. 2 Typical CSI processing flow.

of the transmitter and receiver.

- **SFO:** Because pilot signals are processed by the receiver one by one for each subcarrier, delays are accumulated linearly with the processing order of the subcarriers.
- **PDD:** PDD stems from the symbol synchronization module in the receiver after detecting the frame start.
- **Quantization Error:** Analog-to-digital (A/D) conversion in the receiver introduces quantization error, which amplifies the noise originally included in the CSI. The quantization error becomes larger as the signal amplitude decreases.

Many existing works have introduced sophisticated methods to overcome the aforementioned noise factors. Zhuo et al. [11] studied the CSI noise factors with other additional sources and proposed a calibration method to compensate for nonlinear and linear CSI phase errors. In the following sections, we review the primary preprocessing and feature extraction methods. **Figure 2** shows the typical flow of WiFi CSI-based wireless sensing. For a detailed review, interested readers may refer to surveys on WiFi CSI sensing [2], [3], [4], [5].

2.3 Preprocessing for CSI Noise Mitigation

Before extracting features, smoothing can be applied to reduce the random noise of CSI. For example, Refs. [12], [13], [14] employ Svitzky–Golay(SG)–filter for denoising. We note that some methods [12], [15], [16], [17], [18], [19] perform denoising and feature extraction simultaneously by principal component analysis (PCA) and independent component analysis (ICA). Similarly, others [20], [21], [22] use the MUSIC algorithm to extract signals of interests without denoising directly. Therefore, the design of preprocessing and feature extraction should be carefully considered depending on the target context.

2.3.1 Sanitization

A common noise mitigation method is phase sanitization [10], [23], [24], [25], that alleviates SFO and PDD. Because SFO and PDD are linear with sub-carrier indexes, the offset can be estimated by computing its gradient over all subcarriers, as shown in Eq. (4).

If the phase difference between adjacent subcarriers due to SFO and PDD is δ, the CFR of the kth subcarrier is represented as follows:

$$\boldsymbol{H}(f_k, t) = a(f_k, t)e^{-2j\pi f_k(t+\delta(k-1))}, \tag{4}$$

where f_k is the frequency of the k-th subcarrier and $a(f_k, t)$ is the complex attenuation of the k-th subcarrier. As can be seen from Eq. (4), the phase part of the CSI is a function of time. Owing to the linearity of the SFO and PDD phase error on the subcarriers, we can mitigate the error by subtracting the phase difference due to $\delta(k-1)$ for the k-th subcarrier. For simplicity, we define $\theta = f_k(t + \delta(k-1))$. Then, we can apply the least square method to estimate the phase delay y_k of the k-th subcarrier due to SFO and PDD as follows:

$$a = \sum_{k=1}^{S}\left(k - \frac{S}{2}\right)(\theta_k - \bar{\theta})\Big/\sum_{k=1}^{S}\left(k - \frac{S}{2}\right)^2, \tag{5}$$

$$b = \bar{\theta} - a * \frac{S}{2}, \tag{6}$$

$$y_k = a * k + b, \tag{7}$$

where $\bar{\theta}$ is the average of θ of all the subcarriers.

2.3.2 CSI Ratio

In a real environment, a random offset θ_{offset} due to CFO is added, which is represented as

$$H(f, t) = e^{-j\theta_{offset}}H(f, t) \tag{8}$$

To remove the random offset due to CFO, the ratio of CSI between a pair of antennas on the transceiver is used, which cancels out the phase offsets [8], [9]. This is because the antennas of a wireless device (i.e., the transmitter or receiver) are connected to the same oscillator, which results in the same CFO. The CSI ratio $H_{n,m}$ between antennas m and n is defined as follows:

$$H_{n,m}(f, t) = \frac{e^{-j\theta_{offset}}H_n(f, t)}{e^{-j\theta_{offset}}H_m(f, t)} = \frac{H_n(f, t)}{H_m(f, t)} \tag{9}$$

We note that the CSI ratio can be defined between the antenna pairs of the receiver and transmitter. Therefore, the CSI ratio is $({}_{N_{T_x}*N_{R_x}}C_2 * S)$-dimensional data with respect to the number of transmitter antennas N_{T_x}, the number of receiver antennas N_{R_x}, and the number of subcarriers S. Note that ${}_{N_{T_x}*N_{R_x}}C_2$ is the number of T_x and R_x pairs. The CSI ratio still retains the other features, canceling out CFO.

2.4 Feature Extraction

2.4.1 Principal Component Analysis

Reference [26] used PCA to decompose the mixed RF signals into signal changes due to noises and target movements. As studied in Ref. [26], the third component of PCA has the highest human-movement signal-to-noise-ratio (SNR). In this sense, PCA is a method for feature extraction as well as noise filtering.

2.4.2 Independent Component Analysis

Similar to PCA, ICA can be used to separate mixed signals from multiple reflection sources and direct paths. Reference [27] leverages ICA to extract the effect of signals reflected by objects with state change (e.g., opening a door).

2.4.3 Angle-of-Arrival (AoA) Estimation

WiFi-based AoA estimation has been actively studied because AoA is the vital information that provides a real-world context. AoA estimation leverages multiple antennas on the receiver to extract features of interests depending on the targets. MUSIC algorithm is widely used for this purpose [20], [21], [22]. Because the MUSIC algorithm outputs a spatial spectrum function representing the signal amplitude for each arrival angle, it works as a decomposer in terms of signal paths.

Interestingly, FreeSense [21] leverages the MUSIC algorithm

to detect human movement, which is observed as the CSI phase differences at the receiver antennas. Because the MUSIC algorithm has strong anti-interference ability against random noise, FreeSense does not employ any denoising scheme. ArrayTrack [28] is a CSI-based indoor positioning system that utilizes the MUSIC algorithm to estimate AoA with multiple antennas. SpotFi [29] is also a CSI-based indoor positioning system; it calculates both AoA and time-of-flight (ToF) at the same time with the MUSIC algorithm. ROArray [30] is a CSI-based indoor positioning system that employs sparse recovery to retrieve AoA information even under a low SNR.

2.4.4 Doppler Frequency Shift

Doppler frequency shift (DFS) is one of the key features for human context recognition because it can infer the moving speed of the target. After signal selection (e.g., MUSIC algorithm), the DFS of the signal is extracted based on its phase change. This may work well for sensing contexts such as breathing and gestures of relatively static (e.g., sitting and sleeping) targets. WiPolar [31] proposed a simultaneous estimation of the direction of the target (i.e., signal selection) and DFS to overcome the challenge when the target is moving.

2.4.5 Deep Neural Network

Deep neural networks (DNNs) such as convolutional neural networks (CNNs) are another trend for feature extraction, similar to other research domains [13], [27], [32], [33], [34]. Using a large amount of training data, a DNN has the capability to learn models that are difficult for humans to explain. However, a major concern is that learned models are often environment- and subject-dependent, which creates new challenges for practical applications.

2.4.6 Transfer Learning

To reduce the cost of collecting training data, several studies used transfer learning for CSI-based context recognition. For example, Rao et al. [35] employed transfer learning for CSI-based indoor positioning to learn feature representations such as fingerprints by minimizing the distribution differences between a fingerprint database and test samples. Bu et al. [36] converted CSI data into image data and pre-trained an activity recognition model using a public image dataset for object recognition (ImageNet). Arshad et al. [37] also employed pre-trained image-based neural networks for multiple human activity recognition. Jiang et al. [38] employed domain-adversarial training for activity recognition, whereas Wang et al. [39] employed domain-adversarial training for in-car activity recognition.

2.5 Tools to Obtain CSI

The use of special customized hardware such as USRP [40] and WARP [41] enables the extraction of more detailed physical space information than CSI. However, the use of commercially available equipment such as IEEE 802.11n is advantageous for deployment and the reproducibility of research results. In particular, the emergence of CSI tools [42], [43], [44], [45] has been particularly significant for the wireless sensing research community. Commercially available IEEE 802.11n devices not only produce various research results, but they have also opened up possibilities for the deployment of wireless sensing. However, at present, research using IEEE 802.11n faces the problem that only one section of IEEE 802.11n devices, Intel 5300 NIC, Atheros AR9390, AR9580, AR9590, AR9344, or QCA9558, can obtain CSI. One of the promising options is the IEEE 802.11ac [46], [47] compressed CSI. The IEEE 802.11ac compressed CSI is standardized to reduce the overhead of CSI feedback. Compressed CSI can be acquired from any device that supports IEEE 802.11ac or IEEE 802.11ax. Furthermore, the ESP32 CSI Toolkit [48] is another option to obtain CSI directly from the ESP32 microcontroller, enabling CSI data collection from a large number of tiny IoT devices.

2.6 Applications

In this section, we briefly describe the recent literature on wireless sensing by WiFi CSI. **Table 1** summarizes our review.

2.6.1 Activity Recognition

In Ref. [26], the authors proposed two models for quantitatively correlating CSI dynamics and human activities: a CSI-speed model that correlates CSI dynamics with the movement speed and a CSI-activity model that correlates the movement speed of different body parts with a specific activity. Gao et al. [59] converted CSI measurements from multiple channels into an image and then recognized human activities by extracting color and texture features from the image. Chen et al. [60] recognized human activities by feeding CSI measurements into a neural network with a bidirectional long short-term memory (LSTM) layer. WiStep [57] counted steps based on the CSI energy of the frequency components. For this purpose, WiStep converts CSI to time-domain channel impulse response by inverse fast Fourier transform (IFFT) to remove non-relevant multipath signals. CARIN [50] recognized driver activities using average Doppler shift power with a hidden Markov model-based classification.

2.6.2 Fall Detection

Device-free fall detection for elder care support is another typical application of WiFi CSI. For example, the WiFall system proposed in Ref. [61] employed the time variability and spatial diversity of CSI to detect falls in residential settings, whereas Anti-Fall [62] employed the CSI phase difference over two antennas and used amplitude information to distinguish the fall activity from fall-like activities. FallDeFi [56] extracted the spectrogram of CSI by short-time Fourier transform (STFT) combined with noise filtering by PCA and discrete wavelet transform (DWT) for accurate fall detection.

2.6.3 Vital Sensing

In Ref. [63], the authors attempted to capture user sleep information such as respiration based on WiFi CSI by extracting rhythmic patterns associated with respiration. MultiSense [15] achieved the respiration monitoring of multiple persons using ICA to separate mixed signals. It also employed time-varying phase offset cancellation, background static signal removal, and subcarrier selection. FarSense [9] used the CSI ratio for noise cancellation and achieves the respiration monitoring of the target. For robust respiration monitoring, FullBreathe [14] proposed complementarity of CSI amplitude and phase, which are extracted as the conjugate multiplication of CSI between two an-

Table 1 Summary of wireless sensing by WiFi CSI.

Method	Features	Algorithm	Context	Performance
Widar3.0 [32]	Velocity profiles of gestures	Model-based feature extraction and DNN for recognition	Gesture	82.6%-92.4% for cross-domain recognition
WiBorder [49]	DCM-CSI	Model-based	Boundary crossing	99.4% detection rate
MultiSense [15]	ICA	Matching algorithm	Respiration of multiple persons	Error rate of 0.73 bpm (breaths per minute)
WiPolar [31]	AoA, ToF, and DFS	pSAGE algorithm	Multi-person tracking	Median tracking error of 56cm (up to 5 people)
CARIN [50]	Average Doppler shift power	HMM-based classification	Driver activities under interference of passengers (e.g. continuous head nodding)	F1 score of 90.9%
LiquidSense [16]	PCA and resonance frequencies	SVM classification for discrete liquid level. Curvilinear regression for continuous liquid level.	Liquid level	97% accuracy
FingerDraw [51]	CSI quotient	CSI-quotient model	Sub-wavelength level finger motion tracking	Median tracking accuracy of 1.27cm, 93% accuracy in recognition of drawing ten digits
FarSense [9]	CSI ratio	Model-based	Respiration	Mean absolute error of 0.34bpm in through-wall respiration sensing
WiDetect [52]	ACF of the CSI power response	Hypothesis testing	Motion detection covering whole house/office floor	99.5% detection rate with 0.1% false alarm
WIO [12]	Acceleration and CSI PCA (SG-filter for denoising)	Fusion by Kalman filter	Indoor odometer (traversed distance)	6.87% relative odometer error
Zhang et al. [13]	CSI amplitude denoised by SG-filter	CNN; FFZ Diffraction model	Repetitive activities in FFZ	95+% precision and recall for push-up, sit-up, and walkout
Guo et al. [33]	CSI autocorrelation	DNN models for individual identification and exercise recognition. Spectrogram-based workout detection algorithm	Device-free individual identification and workout assessment (repetition tempo ratio and work-to-rest ratio)	93% accuracy on workout recognition and 97% accuracy for individual detection (20 subjects, 10 exercises)
WiVit [20]	CSI phase change and path-length change speed	Model-based speed estimation	Training-free vitality sensing	98+% precision of activity detection and almost 100% of area detection accuracy
WiID [17]	Spectrogram of CSI denoised by PCA	Machine-learning based model for gesture and user classification	User authentication by gesture	92.8% accuracy for 5 users
FreeSense [21]	Phase difference	Peak detection	Indoor human detection	False positive rate of 0.53%, false negative rate of 1.4%
FullBreathe [14]	Conjugate multiplication of CSI	FFT	Respiration	100% detection rate if a subject faces the transceivers
SiFi [53]	Time of Arrival (ToA)	Hankel matrix decomposition and clustering	Localization	Median accuracy of 0.93m
SignFi [34]	Sanitized CSI amplitude and phase	CNN	276 gestures of sign language	94+% accuracy for 276 gestures by a single user; 86.66% for 150 sign gestures by 5 users
Zhang et al. [54]	Phase change	FFZ diffraction model	Respiration	98+% accuracy
QGesture [55]	Sanitized CSI phase; PCI for subcarrier selection; PCA for phase information recovery	Model-based	Gesture distance and direction	3.7 cm moving distance error, 15 degrees moving direction error
FallDeFi [56]	CSI spectrogram; Discrete Wavelet Transform (DWT) for denoising	SVM classifier	Fall detection	93% accuracy for pre-trained environment, 80% accuracy for different environment
WiStep [57]	CSI energy of frequency components	Model-based	Step count	87.59%-90.2% counting accuracies
Rapid [58]	CSI and acoustic information	Machine learning with hand-crafted features	Person identification	92% to 82 % accuracy from a group of 2 to 6 subjects
Ohara et al. [18]	ICA and DNN	Hiden Markov Model	State changes of indoor objects (open/close door/window/shade, etc.)	85% accuracy
WiMu [19]	PCA-based denoising; Frequency feature by STFT	Database matching	Multi-user gesture recognition	90+% accuracy for 2-6 simultaneous gestures
Strobe [22]	Relative Time of Flight (ToF); AoA estimation by MUSIC	Model-based	Soil moisture and electrical conductivity (EC)	Comparable accuracy with expensive soil sensors

tennas. Zhang et al. [54] proposed respiration sensing by phase change based on a first Fresnel zone (FFZ) diffraction model.

2.6.4 Localization and Tracking

WiPolar [31] proposed multi-person tracking by simultaneously estimating AoA, ToF, and DFS using the extended space-alternating generalized expectation-maximization algorithm called pSAGE. WIO [12] estimated indoor odometry by fusion of acceleration and CSI. SiFi [53] estimated the ToA from CSI by using Hankel matrix decomposition.

2.6.5 Human Detection

Lv et al. [64] detected an intruder using WiFi CSI by extracting a robust feature with continuous wavelet transform. WiBorder [49] detected boundary crossing based on DCM-CSI: CSI conjugate multiplication between two antennas. WiDetect [52] succeeded in motion detection covering a whole house and office floor using the autocorrelation function of the power response of CSI. WiVit [20] is a method for training-free vitality sensing (i.e., whether a target is still or not, moving speed, and its area). It employed CSI phase change of dynamic path signals for activity detection and path-length change speed for area detection. FreeSense [21] leveraged the MUSIC algorithm to estimate the phase difference due to human movement for indoor human detection. It performs peak detection for a spatial spectrum function output using MUSIC.

2.6.6 Human Identification/Authentication

WiID [17] proposed user authentication by gestures using CSI based on machine learning with a CSI spectrogram (i.e., frequency spectrum over time) obtained by STFT. Rapid [58] combines CSI and acoustic signals to achieve accurate person identification. IFFT is employed to remove the multipath effect.

2.6.7 Gesture Recognition

Widar3.0 [32] recognized gestures by extracting body-coordinate velocity profiles based on estimated body orientation to achieve cross-domain recognition. FingerDraw [51] achieved sub-wavelength-level finger motion tracking without attaching any sensor to the finger. It leveraged the CSI quotient between two antennas of a receiver to cancel out the noise and offsets. The CSI-quotient model was used to describe the connection between the motion displacement and CSI variations. SignFi [34] recognized 276 gestures of a sign language using sanitized CSI input to the CNN. For recognition of gesture distance and direction, QGesture [55] employed principal component identification for subcarrier selection and PCA for phase information recovery. WiMu [19] succeeded in multi-user gesture recognition using frequency features extracted by STFT.

2.6.8 Fitness Monitoring

Zhang et al. [13] recognized repetitive activities such as pushups by focusing on the model of the FFZ. The FFZ model was used to guide system deployment. Guo et al. [33] achieved individual identification and workout assessment using CSI autocorrelation and DNN.

2.6.9 Object Event Detection

Ohara et al. [18] employed WiFi CSI to recognize events of everyday objects, including door open/close events. A deep learning model was used to automatically extract efficient classification features. Xu et al. [65] employed WiFi CSI to recognize door events based on features extracted from CFR and a classifier using dynamic time warping.

2.6.10 Material/Moisture Sensing

LiquidSense [16] estimated the liquid level in a container using a transducer attached to the surface of a cup. It captured the liquid-level dependent vibration generated by a transducer on the surface of a cup using CSI. WiFi CSI is also capable of soil moisture sensing as presented in Strobe [22], which exploits the relative ToF. The multipath signals were removed using the MUSIC algorithm. Because Strobe used multiple Rx antennas, PDD, SFO, and CFO were canceled out.

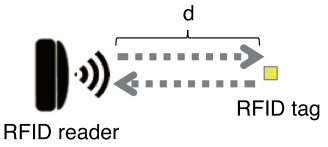

Fig. 3 Basic principle of RFID sensing.

3. RFID Sensing

3.1 Overview of Wireless Sensing by RFID

The RFID system is composed of a reader and battery-less tags [*1]. The RFID reader emits a continuous wave (CW) signal to provide passive tags with energy. The tags send back data such as their identification by backscatter communication. Backscatter communication is ultra-low power because it leverages CW from the reader without generating a high-frequency active RF signal, which requires a large amount of energy in many devices.

Commercial RFID systems such as the ImpinJ Speedway RFID reader provide information on the received signal strength (RSS) and phase of the received signal from tags. Although the APIs of the commodity RFID systems provide RSS information, they are usually unstable and unreliable. For this reason, many approaches rely mainly on phase measurement. However, some methods also leverage RSS.

Based on basic physics, the following equation holds between the observed phase θ and distance d between a reader antenna and a tag (see **Fig. 3**).

$$\theta = \left(2\pi\frac{2d}{\lambda} + \theta_n\right) \mod 2\pi, \tag{10}$$

where θ_n is the noise. By observing the phase change over time, we can infer contexts related to the movements of objects.

3.2 Noise Sources and Countermeasures

The primary sources of RFID system noise are tag hardware imperfection, tag antenna orientation, and multipath effect. Furthermore, some countries' regulations, including the U.S., require frequency hopping, which affects the phase-angle measurements.

Tag hardware imperfection is mitigated by calibration, for example, measuring the distance between an antenna and a tag. We note that some methods assume a constant noise for the hardware imperfection without calibration, which can be mitigated by sampling over time and multiple measurements of tags and receiver antennas.

The phase difference between multiple tags is introduced in RF-Kinect [66] to overcome the effect of the antenna orientation. Similarly, the phase difference between multiple reader antennas (i.e., an antenna array) can be used.

Because the multipath effect is more like random noise, Yang and Cao [67] employed a matched filter to separate a known signal template (e.g., repetitive pattern of respiration) from the multipath signals. Furthermore, similar to CSI, TagFree [68] performs AoA estimation by the MUSIC algorithm to identify the

[*1] We focus on passive RFID tags owing to its unique nature of battery-free operation, although other types of active RFID tags are also available.

Table 2 Summary of wireless sensing by RFID.

Method	Features	Algorithm	Reader	Tag	Context	Performance
RF-Kinect [66]	Phase Difference Between Tags (PDT)	Model-based	1 reader with 2 antennas	Multiple Tags on body	3D body movement	8.7 degree limb angle error and 4.4cm relative joint position error
TagFree [68]	AoA change over time (AoA spectrum)	Deep learning (CNN+LSTM)	1 reader with 4 antennas	6 tags on furniture	7 activities: stand, sit, wave, bow, walk, run, work	91%-97% average accuracy, depends on activity speed and multipath environment
EUIGR [70]	Phase and RSS	Deep learning (CNN+LSTM)	1 reader with 1 antenna	2 tags attached on each arm	8 traffic command gestures	96% precision and recall with unseen users; 88.6% precision and 86.7% recall in untrained positions
Yang and Cao [67]	Phase	Matched filtering	1 reader with 1 antenna	1 tag on chest	Respiration monitoring	0.5 bpm error for respiration rate; 5.3% error for apnea detection
Tagtag [71]	Material-dependent phase change	Dynamic Time Warping	1 reader with 1 antenna	2 tags on container	Material Sensing	90+% accuracy even for similar materials like Pepsi and Coke
Li et al. [72]	RSS	CNN	2 readers, 8 antennas	12 tags on 12 objects	11 Medical and 6 lab activity recognition	80.4% accuracy for medical activities, 90.8% for lab activities
ShopMiner [73]	Phase	Model-based	1 reader with 4 antennas	One tag on each item	Turn item over, pick item up	87+% accuracy
FEMO [74]	Phase (Doppler shifts)	Fingerprint matching by Dynamic Time Warping	1 reader with 1 directional antenna	2 tags on dumbbells	10 free-weight activities	90% precision and 91% recall
RFID Tattoo [75]	RSS and phase (impedance change due to stretch of tags)	Classification by machine learning (Random Forest)	1 reader with 1 antenna on user 窶ｵ waist	4 stretchable customized tags around mouth	Speech recognition	86% accuracy in reconstructing the top-100 words in English
ER-Rhythm [76]	Phase	Model-based	1 reader with 1 or 2 antennas	tags on the limbs and front and back chest	LRC ratio	Accurate estimation up to 92%-95% of the exercise duration
LungTrack [77]	RSS and phase	Fresnel diffraction and reflection models	1 reader with 1 antenna	5 tags near the subject	Respiration monitoring	98% accuracy for a single target, 93% accuracy for two subjects separated by at least 10cm
TagSleep [78]	Phase; time-domain, frequency-domain and sample entropy features	Classification by machine learning	1 reader with 1 antenna	3 tags near the subject	Respiration and snore, cough, and somniloquy	96.58+% accuracy in recognizing snore, cough, and somniloquy
AdaRF [79]	Phase (simulation and experiment)	CNN with transfer learning	1 reader with 1 moving antenna	1 tag on each object	Localization	cm-level positioning
Au-Id [80]	Phase and RSSI	CNN and LSTM	1 reader with 1 antenna	3x3 tag array on the door	User identification and authentication	94.2% identification accuracy (15 users), 96.11% authentication accuracy (8 legitimate users and 7 spoofers)
RF-Focus [69]	Phase, RSSI, and images	Model-based distance estimation and matching	1 reader with 2 antennas	1 tag on each object	Tag locations in Region of Interest (ROI)	True positive rates of 91.6% and false positive rates of 10%
TACT [81]	Moving speed, moving distance, activity duration estimated by phase, and phase waveform	Machine-learning based classifier	1 reader with 1 antenna	4 tags near the subject (Reader-tag distance=2m-4m)	8 human activities (stand, sit, raisehand, drophand, walk, fall, rotation, get-up)	93.5% precision
RF-ECG [82]	Chest movement estimation by phase change	Model-based; DWT-based denoising	1 reader with 1 antenna in front of the subject	tag array on the chest	Heart rate variability	Median error of 3% of Inter-Beat Interval (IBI)
RF-Copybook [83]	Phase; random noise filtering by Kalman filter	Model-based distance estimation	1 reader with 3 antennas	2 tags on a brush	Chinese calligraphy monitoring	4.8mm-7.5mm distance estimation errors depending on multipath environment
RF-Wear [84]	Phase	Model-based	1 reader with 1 antenna in a pocket	tag arrays (matrixes) on each joint	Body pose	Mean error of 8-21 degrees in tracking angles at joints
Wang et al. [85]	Differential Minimum Response Threshold (DMRT)	Model-based	1 reader with 1 antenna over pots	2 tags on each pot	Soil moisture	90-percentile moisture estimation errors of 5%

signal reflected from the human body. Such signal path selection methods are useful to focus on the signals of interests.

3.3 Applications

Wireless sensing by RFID systems is roughly classified into *tagged approaches* and *device-free approaches*. In the tagged approaches, RFID tags are attached to the subjects/objects of interest to directly sense the movement of the tagged parts. This is the major difference between RFID and WiFi CSI: RFID tags are attached to the targets, and the reader can distinguish the source tag of the received signal from other tags. Some studies have also proposed device-free approaches where tags are deployed in the proximity of the targets (e.g., doors and beds). The nature of the identification capability of RFID systems provides a clear separation of the signal sources (i.e., tags), which enables us to capture more precise movement than WiFi CSI-based wireless sensing.

Table 2 summarizes our review on the recent RFID-based wireless sensing. We note that a fusion of RFID with other sensors is another option for enhancing its capability. One of such methods is RF-Focus [69], which combined RFID and a camera to precisely estimate tag locations in the region of interest.

3.3.1 Tagged Approach

RF-Kinect [66] recognized three-dimensional (3D) body movements by attaching multiple tags to the subject's body. It employed a phase difference between tags (PDT) to track the body movement, which is robust to antenna orientation change. RF-Wear [84] recognized body pose with tag arrays on each joint by observing the phase difference between the signals from the tags.

To achieve real-time gesture recognition, EUIGR [70] proposed an LSTM-based sequence labeling classifier that predicts gestures before its completion using two tags attached to each arm. RFID Tattoo [75] proposed the design of stretchable customized tags; the tags were attached to the upper and lower jaws and two sides of the mouth for speech recognition. The tag antenna impedance changes due to the stretch of tags related to the movement of the mouth.

ShopMiner [73] tracked customer behavior such as turning the item over and picking the item up by tags attached to each item. AdaRF [79] used a CNN with transfer learning for localization of tagged targets, achieving cm-level positioning. Li et al. [72] employed a CNN to recognize 11 medical and 6 lab activities (e.g., oxygen preparation, blood pressure measurement, and lab-meeting.) by tags attached to objects. RF-Copybook [83] achieved millimeter-level antenna-tag distance estimation for Chinese calligraphy monitoring by two tags on a brush. RF-Copybook used a Kalman filter to filter random noise. In addition, the phase shift due to tag imperfection was calibrated by measuring the distance between the antenna and tag.

Yang and Cao [67] proposed respiration monitoring with a tag attached to the chest by finding continuous breathing patterns from a signal with a multipath effect by matched filtering. ER-Rhythm [76] estimated the locomotor–respiratory coupling (LRC) ratio, which is the correlation between exercise locomotion and respiration rhythm. RF-ECG [82] estimated heart rate variability with a tag array attached to the chest by separating chest movement due to respiration and heartbeat. FEMO [74] recognized ten free-weight activities by two tags attached to dumbbells.

Interestingly, Tagtag [71] is a method for material sensing using two tags on a container, leveraging material-dependent phase change (i.e., antenna impedance changes). In addition, soil moisture sensing is possible by attaching two tags on each pot based on the signal change due to soil moisture [85].

3.3.2 Device-Free Approach

TagFree [68] attached multiple tags on furniture to recognize seven human activities using deep learning. It used AoA change over time (AoA spectrum), representing the change of backscattered signal paths related to target activities. LungTrack [77] employed Fresnel diffraction and reflection models for respiration monitoring with five tags deployed near the subject. TagSleep [78] is a device-free approach for the recognition of respiration and snoring, cough, and somniloquy. It also employed a wavelet filter to remove high-frequency noise. AuId [80] achieved user identification and authentication with CNN and LSTM using a 3×3 tag array on the door. TACT [81] recognized eight activities with four tags near the subject by extracting various features such as moving speed, distance, activity duration, and phase waveform.

4. Backscatter Sensing

Backscatter sensing is a novel yet classical concept of battery-free or ultra-low-power sensing by direct conversion of contexts into backscattered signal changes. The basic concept is similar to some classic devices such as the Great Seal Bug [86] and a laser microphone [87]—backscattering signals from an external source in a passive manner.

Printed WiFi [88] is one of the emerging concepts of recent backscatter sensing. It directly converts contexts such as wind speed, liquid flow, the moving distance of a slider bar, and the amount of knob rotation into the variation of backscattered WiFi signals without any digital modulation. LiveTag [89] is a printed tag composed of two antennas and resonators. The resonator absorbs the WiFi signal of a specific frequency, which is used for the identification of the resonators. Based on this principle, LiveTag [89] leveraged the cancellation of the resonator effect by finger touch and liquid to enable battery-less touchpads and liquid-level sensing.

The aforementioned two approaches are entirely battery-free, without any silicon chips. On the contrary, a tiny amount of energy (e.g., harvested from ambient light) broadens the capability of backscatter sensing. BARNET [90] proposed backscatter channel state information between backscatter tags to obtain activity-related signal change information similar to WiFi CSI. Because backscatter tags can be deployed anywhere without the limitation of batteries, the number of backscatter tag-to-tag links is expected to be much higher than that of WiFi CSI. Therefore, we can expect wide area coverage and more robust context recognition. RF Bandaid [91] proposed an RF sensing platform that consists of an energy harvester, an antenna, an oscillator, an RF switch, and a resistive or capacitive sensor. The resistive or capacitive sensor changes its resistance or capacitance according

to its sensing target. For example, the capabilities of temperature, force, and stress measurements have been demonstrated in Ref. [91]. RF Bandaid employed a micropower precision programmable oscillator from Linear Technology LTC6906. This oscillator converts the resistance or capacitance of the sensor to a specific frequency. The RF switch changes its state according to the oscillator frequency, resulting in a frequency shift in the backscattered signal. The concept of a touchpad using FM backscatter was presented in UbiquiTouch [92], which modulates a touch point on a surface to its corresponding time-series pattern of the frequency shift. OFDMA backscatter localization with ultra-low power was also proposed in Ref. [93] using an extended MUSIC algorithm.

5. Design Choice of Wireless Sensing

As we reviewed, wireless sensing by WiFi CSI is the mainstream of the research because of its wide availability. RFID sensing has also been attracting the attention of many researchers owing to its nature of identification and ubiquitous tags. Backscatter sensing is similar to RFID sensing; however, customized tags are used to more directly recognize contexts.

The design choice of wireless sensing depends on various requirements such as deployment cost, target context, and required performance. WiFi sensing has a great advantage in deployment cost, whereas the target environment and performance may be limited. By contrast, RFID sensing can typically achieve higher accuracy than WiFi CSI because it provides signals from many tags that are even attachable to the targets. Backscatter sensing further enhances the capability of wireless sensing by directly converting context into ambient RF signal change such as WiFi and BLE; however it requires careful design of customized tags.

6. Conclusion

In this study, we comprehensively reviewed wireless sensing by WiFi CSI, RFID, and backscatter. Wireless sensing has a wide variety of applications owing to its pervasive and ubiquitous nature. We also provided the design choice of wireless sensing, depending on the requirements. We hope that this review will help researchers open up new research directions for wireless sensing.

Acknowledgments This work was partly supported by JST, PRESTO Grant Number JPMJPR1932, and JSPS KAKENHI 19K11941, JP20K20398, and JP19H05665, Japan.

References

[1] Liu, V., Parks, A., Talla, V., Gollakota, S., Wetherall, D. and Smith, J.R.: Ambient Backscatter: Wireless Communication out of Thin Air, *SIGCOMM Comput. Commun. Rev.*, Vol.43, No.4, pp.39–50 (online), DOI: 10.1145/2534169.2486015 (2013).

[2] Wang, Z., Jiang, K., Hou, Y., Dou, W., Zhang, C., Huang, Z. and Guo, Y.: A Survey on Human Behavior Recognition Using Channel State Information, *IEEE Access*, Vol.7, pp.155986–156024 (2019).

[3] Ma, Y., Zhou, G. and Wang, S.: WiFi Sensing with Channel State Information: A Survey, *ACM Comput. Surv.*, Vol.52, No.3 (online), DOI: 10.1145/3310194 (2019).

[4] Yousefi, S., Narui, H., Dayal, S., Ermon, S. and Valaee, S.: A Survey on Behavior Recognition Using WiFi Channel State Information, *IEEE Communications Magazine*, Vol.55, No.10, pp.98–104 (2017).

[5] Liu, J., Liu, H., Chen, Y., Wang, Y. and Wang, C.: Wireless Sensing for Human Activity: A Survey, *IEEE Communications Surveys Tutorials*, Vol.22, No.3, pp.1629–1645 (2020).

[6] Yuan, J. and Torlak, M.: Joint CFO and SFO estimator for OFDM receiver using common reference frequency, *IEEE Trans. Broadcasting*, Vol.62, No.1, pp.141–149 (2016).

[7] Tang, X. and Fu, G.: A ML-Based High-Accuracy Estimation of Sampling and Carrier Frequency Offsets for OFDM Systems, *Proc. Springer Computer Engineering and Technology*, Vol.592, p.85 (2016).

[8] Tai, T.-C., Lin, K.C.-J. and Tseng, Y.-C.: Toward Reliable Localization by Unequal AoA Tracking, *Proc. 17th Annual International Conference on Mobile Systems, Applications, and Services*, pp.444–456 (2019).

[9] Zeng, Y., Wu, D., Xiong, J., Yi, E., Gao, R. and Zhang, D.: FarSense: Pushing the Range Limit of WiFi-based Respiration Sensing with CSI Ratio of Two Antennas, *ACM on Interactive, Mobile, Wearable and Ubiquitous Technologies*, Vol.3, No.3, p.121 (2019).

[10] Yousefi, S., Narui, H., Dayal, S., Ermon, S. and Valaee, S.: A Survey on Behavior Recognition using WiFi Channel State Information, *IEEE Communications Magazine*, Vol.55, No.10, pp.98–104 (2017).

[11] Zhuo, Y., Zhu, H., Xue, H. and Chang, S.: Perceiving Accurate CSI Phases with Commodity WiFi Devices, *IEEE INFOCOM 2017 - IEEE Conference on Computer Communications*, pp.1–9 (2017).

[12] Venkatnarayan, R.H. and Shahzad, M.: Enhancing Indoor Inertial Odometry with WiFi, *Proc. ACM Interact. Mob. Wearable Ubiquitous Technol.*, Vol.3, No.2 (online), DOI: 10.1145/3328918 (2019).

[13] Zhang, F., Niu, K., Xiong, J., Jin, B., Gu, T., Jiang, Y. and Zhang, D.: Towards a Diffraction-Based Sensing Approach on Human Activity Recognition, *Proc. ACM Interact. Mob. Wearable Ubiquitous Technol.*, Vol.3, No.1 (online), DOI: 10.1145/3314420 (2019).

[14] Zeng, Y., Wu, D., Gao, R., Gu, T. and Zhang, D.: FullBreathe: Full Human Respiration Detection Exploiting Complementarity of CSI Phase and Amplitude of WiFi Signals, *Proc. ACM Interact. Mob. Wearable Ubiquitous Technol.*, Vol.2, No.3 (online), DOI: 10.1145/3264958 (2018).

[15] Zeng, Y., Wu, D., Xiong, J., Liu, J., Liu, Z. and Zhang, D.: MultiSense: Enabling Multi-Person Respiration Sensing with Commodity WiFi, *Proc. ACM Interact. Mob. Wearable Ubiquitous Technol.*, Vol.4, No.3 (online), DOI: 10.1145/3411816 (2020).

[16] Ren, Y., Tan, S., Zhang, L., Wang, Z., Wang, Z. and Yang, J.: Liquid Level Sensing Using Commodity WiFi in a Smart Home Environment, *Proc. ACM Interact. Mob. Wearable Ubiquitous Technol.*, Vol.4, No.1 (online), DOI: 10.1145/3380996 (2020).

[17] Shahzad, M. and Zhang, S.: Augmenting User Identification with WiFi Based Gesture Recognition, *Proc. ACM Interact. Mob. Wearable Ubiquitous Technol.*, Vol.2, No.3 (online), DOI: 10.1145/3264944 (2018).

[18] Ohara, K., Maekawa, T. and Matsushita, Y.: Detecting State Changes of Indoor Everyday Objects Using Wi-Fi Channel State Information, *Proc. ACM Interact. Mob. Wearable Ubiquitous Technol.*, Vol.1, No.3 (online), DOI: 10.1145/3131898 (2017).

[19] Venkatnarayan, R.H., Page, G. and Shahzad, M.: Multi-User Gesture Recognition Using WiFi, *Proc. 16th Annual International Conference on Mobile Systems, Applications, and Services*, MobiSys '18, pp.401–413, Association for Computing Machinery (online), DOI: 10.1145/3210240.3210335 (2018).

[20] Wang, Y. and Zheng, Y.: Modeling RFID Signal Reflection for Contact-Free Activity Recognition, *Proc. ACM Interact. Mob. Wearable Ubiquitous Technol.*, Vol.2, No.4 (online), DOI: 10.1145/3287071 (2018).

[21] Xin, T., Guo, B., Wang, Z., Wang, P., Lam, J.C.K., Li, V. and Yu, Z.: FreeSense: A Robust Approach for Indoor Human Detection Using Wi-Fi Signals, *Proc. ACM Interact. Mob. Wearable Ubiquitous Technol.*, Vol.2, No.3 (online), DOI: 10.1145/3264953 (2018).

[22] Ding, J. and Chandra, R.: Towards Low Cost Soil Sensing Using Wi-Fi, *The 25th Annual International Conference on Mobile Computing and Networking, MobiCom '19* (online), DOI: 10.1145/3300061.3345440 (2019).

[23] Wang, X., Gao, L. and Mao, S.: PhaseFi: Phase Fingerprinting for Indoor Localization with a Deep Learning Approach, *Proc. IEEE Global Communications Conference* (*GLOBECOM*), pp.1–6 (2015).

[24] Gjengset, J., Xiong, J., McPhillips, G. and Jamieson, K.: Phaser: Enabling Phased Array Signal Processing on Commodity WiFi Access Points, *Proc. 20th Annual International Conference on Mobile Computing and Networking*, pp.153–164 (2014).

[25] Hua, J., Sun, H., Shen, Z., Qian, Z. and Zhong, S.: Accurate and Efficient Wireless Device Fingerprinting using Channel State Information, *Proc. IEEE International Conference on Computer Communications* (*INFOCOM*), pp.1700–1708 (2018).

[26] Wang, W., Liu, A.X., Shahzad, M., Ling, K. and Lu, S.: Understanding and Modeling of WiFi Signal Based Human Activity Recognition, *Proc. 21st Annual International Conference on Mobile Computing and Networking, MobiCom '15*, pp.65–76 (online), DOI: 10.1145/

2789168.2790093 (2015).
[27] Ohara, K., Maekawa, T. and Matsushita, Y.: Detecting State Changes of Indoor Everyday Objects Using Wi-Fi Channel State Information, *Proc. ACM on Interactive, Mobile, Wearable and Ubiquitous Technologies* (*ACM IMWUT'17*), pp.88:1–88:28 (2017).
[28] Xiong, J. and Jamieson, K.: Arraytrack: A Fine-grained Indoor Location System, *The 10th USENIX Symposium on Networked Systems Design and Implementation* (*NSDI*), pp.71–84 (2013).
[29] Kotaru, M., Joshi, K., Bharadia, D. and Katti, S.: Spotfi: Decimeter Level Localization using WiFi, *The 2015 ACM Conference on Special Interest Group on Data Communication*, pp.269–282 (2015).
[30] Gong, W. and Liu, J.: Robust Indoor Wireless Localization using Sparse Recovery, *2017 IEEE 37th International Conference on Distributed Computing Systems* (*ICDCS*), pp.847–856, IEEE (2017).
[31] Venkatnarayan, R.H., Shahzad, M., Yun, S., Vlachou, C. and Kim, K.-H.: Leveraging Polarization of WiFi Signals to Simultaneously Track Multiple People, *Proc. ACM Interact. Mob. Wearable Ubiquitous Technol.*, Vol.4, No.2 (online), DOI: 10.1145/3397317 (2020).
[32] Zheng, Y., Zhang, Y., Qian, K., Zhang, G., Liu, Y., Wu, C. and Yang, Z.: Zero-Effort Cross-Domain Gesture Recognition with Wi-Fi, *Proc. 17th Annual International Conference on Mobile Systems, Applications, and Services, MobiSys '19*, pp.313–325 (online), DOI: 10.1145/3307334.3326081 (2019).
[33] Guo, X., Liu, J., Shi, C., Liu, H., Chen, Y. and Chuah, M.C.: Device-Free Personalized Fitness Assistant Using WiFi, *Proc. ACM Interact. Mob. Wearable Ubiquitous Technol.*, Vol.2, No.4 (online), DOI: 10.1145/3287043 (2018).
[34] Ma, Y., Zhou, G., Wang, S., Zhao, H. and Jung, W.: SignFi: Sign Language Recognition Using WiFi, *Proc. ACM Interact. Mob. Wearable Ubiquitous Technol.*, Vol.2, No.1 (online), DOI: 10.1145/3191755 (2018).
[35] Rao, X., Li, Z. and Yang, Y.: Device-free Passive Wireless Localization System with Transfer Deep Learning Method, *Journal of Ambient Intelligence and Humanized Computing*, pp.1–17 (2020).
[36] Bu, Q., Yang, G., Ming, X., Zhang, T., Feng, J. and Zhang, J.: Deep Transfer Learning for Gesture Recognition with WiFi Signals, *Personal and Ubiquitous Computing*, pp.1–12 (2020).
[37] Arshad, S., Feng, C., Yu, R. and Liu, Y.: Leveraging Transfer Learning in Multiple Human Activity Recognition Using WiFi Signal, *IEEE 20th International Symposium on A World of Wireless, Mobile and Multimedia Networks* (*WoWMoM*), pp.1–10 (2019).
[38] Jiang, W., Miao, C., Ma, F., Yao, S., Wang, Y., Yuan, Y., Xue, H., Song, C., Ma, X., Koutsonikolas, D., et al.: Towards Environment Independent Device Free Human Activity Recognition, *The 24th Annual International Conference on Mobile Computing and Networking*, pp.289–304 (2018).
[39] Wang, F., Liu, J. and Gong, W.: WiCAR: WiFi-based In-car Activity Recognition with Multi-adversarial Domain Adaptation, *International Symposium on Quality of Service*, pp.1–10 (2019).
[40] Ettus Research: USRP, (online), available from ⟨https://www.ettus.com⟩ (accessed 2020-10-05).
[41] Khattab, A., Camp, J., Hunter, C., Murphy, P., Sabharwal, A. and Knightly, E.W.: WARP: A Flexible Platform for Clean-Slate Wireless Medium Access Protocol Design, *ACM SIGMOBILE Mobile Computing and Communications Review*, Vol.12, No.1, pp.56–58 (2008).
[42] Halperin, D., Hu, W., Sheth, A. and Wetherall, D.: Tool Release: Gathering 802.11n Traces with Channel State Information, *ACM SIGCOMM Computer Communication Review*, Vol.41, No.1, p.53 (2011).
[43] Xie, Y., Li, Z. and Li, M.: Precise Power Delay Profiling with Commodity WiFi, *Proc. 21st Annual International Conference on Mobile Computing and Networking* (*ACM MobiCom'15*), pp.53–64 (2015).
[44] Halperin, D., Hu, W., Sheth, A. and Wetherall, D.: Linux 802.11n CSI Tool, (online), available from ⟨https://dhalperi.github.io/linux-80211n-csitool/⟩ (accessed 2020-10-05).
[45] Li, M. and Xie, Y.: Atheros CSI Tool (online), available from ⟨https://wands.sg/research/wifi/AtherosCSI/⟩ (accessed 2020-10-05).
[46] Perahia, E. and Stacey, R.: Next Generation Wireless LANs: 802.11n and 802.11ac, Cambridge University Press (2013).
[47] IEEE: IEEE Standard for Information Technology–Telecommunications and Information Exchange Between Systems Local and Metropolitan Area Networks–Specific Requirements - Part 11: Wireless LAN Medium Access Control (MAC) and Physical Layer (PHY) Specifications, IEEE Std 802.11-2016 (Revision of IEEE Std 802.11-2012), pp.1–3534 (2016).
[48] Hernandez, S.M. and Bulut, E.: Lightweight and Standalone IoT based WiFi Sensing for Active Repositioning and Mobility, *21st International Symposium on A World of Wireless, Mobile and Multimedia Networks* (*WoWMoM*) (2020).
[49] Li, S., Liu, Z., Zhang, Y., Lv, Q., Niu, X., Wang, L. and Zhang, D.: WiBorder: Precise Wi-Fi Based Boundary Sensing via Through-Wall Discrimination, *Proc. ACM Interact. Mob. Wearable Ubiquitous Technol.*, Vol.4, No.3 (online), DOI: 10.1145/3411834 (2020).
[50] Bai, Y. and Wang, X.: CARIN: Wireless CSI-Based Driver Activity Recognition under the Interference of Passengers, *Proc. ACM Interact. Mob. Wearable Ubiquitous Technol.*, Vol.4, No.1 (online), DOI: 10.1145/3380992 (2020).
[51] Wu, D., Gao, R., Zeng, Y., Liu, J., Wang, L., Gu, T. and Zhang, D.: FingerDraw: Sub-Wavelength Level Finger Motion Tracking with WiFi Signals, *Proc. ACM Interact. Mob. Wearable Ubiquitous Technol.*, Vol.4, No.1 (online), DOI: 10.1145/3380981 (2020).
[52] Zhang, F., Wu, C., Wang, B., Lai, H.-Q., Han, Y. and Liu, K.J.R.: WiDetect: Robust Motion Detection with a Statistical Electromagnetic Model, *Proc. ACM Interact. Mob. Wearable Ubiquitous Technol.*, Vol.3, No.3 (online), DOI: 10.1145/3351280 (2019).
[53] Gong, W. and Liu, J.: SiFi: Pushing the Limit of Time-Based WiFi Localization Using a Single Commodity Access Point, *Proc. ACM Interact. Mob. Wearable Ubiquitous Technol.*, Vol.2, No.1 (online), DOI: 10.1145/3191742 (2018).
[54] Zhang, F., Zhang, D., Xiong, J., Wang, H., Niu, K., Jin, B. and Wang, Y.: From Fresnel Diffraction Model to Fine-Grained Human Respiration Sensing with Commodity Wi-Fi Devices, *Proc. ACM Interact. Mob. Wearable Ubiquitous Technol.*, Vol.2, No.1 (online), DOI: 10.1145/3191785 (2018).
[55] Yu, N., Wang, W., Liu, A.X. and Kong, L.: QGesture: Quantifying Gesture Distance and Direction with WiFi Signals, *Proc. ACM Interact. Mob. Wearable Ubiquitous Technol.*, Vol.2, No.1 (online), DOI: 10.1145/3191783 (2018).
[56] Palipana, S., Rojas, D., Agrawal, P. and Pesch, D.: FallDeFi: Ubiquitous Fall Detection Using Commodity Wi-Fi Devices, *Proc. ACM Interact. Mob. Wearable Ubiquitous Technol.*, Vol.1, No.4 (online), DOI: 10.1145/3161183 (2018).
[57] Xu, Y., Yang, W., Wang, J., Zhou, X., Li, H. and Huang, L.: WiStep: Device-Free Step Counting with WiFi Signals, *Proc. ACM Interact. Mob. Wearable Ubiquitous Technol.*, Vol.1, No.4 (online), DOI: 10.1145/3161415 (2018).
[58] Chen, Y., Dong, W., Gao, Y., Liu, X. and Gu, T.: Rapid: A Multimodal and Device-Free Approach Using Noise Estimation for Robust Person Identification, *Proc. ACM Interact. Mob. Wearable Ubiquitous Technol.*, Vol.1, No.3 (online), DOI: 10.1145/3130906 (2017).
[59] Gao, Q., Wang, J., Ma, X., Feng, X. and Wang, H.: CSI-based Device-free Wireless Localization and Activity Recognition using Radio Image Features, *IEEE Trans. Vehicular Technology*, Vol.66, No.11, pp.10346–10356 (2017).
[60] Chen, Z., Zhang, L., Jiang, C., Cao, Z. and Cui, W.: WiFi CSI based Passive Human Activity Recognition using Attention based BLSTM, *IEEE Trans. Mobile Computing*, Vol.18, No.11, pp.2714–2724 (2018).
[61] Han, C., Wu, K., Wang, Y. and Ni, L.M.: WiFall: Device-free Fall Detection by Wireless Networks, *IEEE Conference on Computer Communications* (*INFOCOM 2014*), pp.271–279 (2014).
[62] Zhang, D., Wang, H., Wang, Y. and Ma, J.: Anti-fall: A Non-intrusive and Real-time Fall Detector Leveraging CSI from Commodity WiFi devices, *International Conference on Smart homes and health Telematics* (*ICOST 2015*), pp.181–193 (2015).
[63] Liu, X., Cao, J., Tang, S. and Wen, J.: Wi-Sleep: Contactless Sleep Monitoring via WiFi Signals, *IEEE Real-Time Systems Symposium* (*RTSS 2014*), pp.346–355 (2014).
[64] Lv, J., Man, D., Yang, W., Gong, L., Du, X. and Yu, M.: Robust Device-free Intrusion Detection using Physical Layer Information of WiFi Signals, *Applied Sciences*, Vol.9, No.1, p.175 (2019).
[65] Xu, Q., Han, Y., Wang, B., Wu, M. and Liu, K.R.: Indoor Events Monitoring Using Channel State Information Time Series, *IEEE Internet of Things Journal*, Vol.6, No.3, pp.4977–4990 (2019).
[66] Wang, C., Liu, J., Chen, Y., Xie, L., Liu, H.B. and Lu, S.: RF-Kinect: A Wearable RFID-Based Approach Towards 3D Body Movement Tracking, *Proc. ACM Interact. Mob. Wearable Ubiquitous Technol.*, Vol.2, No.1 (online), DOI: 10.1145/3191773 (2018).
[67] Yang, Y. and Cao, J.: Robust RFID-based Respiration Monitoring in Dynamic Environments, *2020 17th Annual IEEE International Conference on Sensing, Communication, and Networking* (*SECON*), pp.1–9 (2020).
[68] Fan, X., Gong, W. and Liu, J.: TagFree Activity Identification with RFIDs, *Proc. ACM Interact. Mob. Wearable Ubiquitous Technol.*, Vol.2, No.1 (online), DOI: 10.1145/3191739 (2018).
[69] Wang, Z., Xu, M., Ye, N., Wang, R. and Huang, H.: RF-Focus: Computer Vision-Assisted Region-of-Interest RFID Tag Recognition and Localization in Multipath-Prevalent Environments, *Proc. ACM Interact. Mob. Wearable Ubiquitous Technol.*, Vol.3, No.1 (online), DOI: 10.1145/3314416 (2019).
[70] Yu, Y., Wang, D., Zhao, R. and Zhang, Q.: RFID Based Real-Time Recognition of Ongoing Gesture with Adversarial Learning, *Proc. 17th Conference on Embedded Networked Sensor Systems, SenSys '19*, pp.298–310 (online), DOI: 10.1145/3356250.3360045 (2019).

[71] Xie, B., Xiong, J., Chen, X., Chai, E., Li, L., Tang, Z. and Fang, D.: Tagtag: Material Sensing with Commodity RFID, *Proc. 17th Conference on Embedded Networked Sensor Systems, SenSys '19*, pp.338–350 (online), DOI: 10.1145/3356250.3360027 (2019).

[72] Li, X., Zhang, Y., Marsic, I., Sarcevic, A. and Burd, R.S.: Deep Learning for RFID-Based Activity Recognition, *Proc. 14th ACM Conference on Embedded Network Sensor Systems CD-ROM, SenSys '16*, pp.164–175 (online), DOI: 10.1145/2994551.2994569 (2016).

[73] Shangguan, L., Zhou, Z., Zheng, X., Yang, L., Liu, Y. and Han, J.: ShopMiner: Mining Customer Shopping Behavior in Physical Clothing Stores with COTS RFID Devices, *Proc. 13th ACM Conference on Embedded Networked Sensor Systems, SenSys '15*, pp.113–125 (online), DOI: 10.1145/2809695.2809710 (2015).

[74] Ding, H., Shangguan, L., Yang, Z., Han, J., Zhou, Z., Yang, P., Xi, W. and Zhao, J.: FEMO: A Platform for Free-Weight Exercise Monitoring with RFIDs, *Proc. 13th ACM Conference on Embedded Networked Sensor Systems, SenSys '15*, pp.141–154 (online), DOI: 10.1145/2809695.2809708 (2015).

[75] Wang, J., Pan, C., Jin, H., Singh, V., Jain, Y., Hong, J.I., Majidi, C. and Kumar, S.: RFID Tattoo: A Wireless Platform for Speech Recognition, *Proc. ACM Interact. Mob. Wearable Ubiquitous Technol.*, Vol.3, No.4 (online), DOI: 10.1145/3369812 (2019).

[76] Yang, Y., Cao, J. and Liu, X.: ER-Rhythm: Coupling Exercise and Respiration Rhythm Using Lightweight COTS RFID, *Proc. ACM Interact. Mob. Wearable Ubiquitous Technol.*, Vol.3, No.4 (online), DOI: 10.1145/3369808 (2019).

[77] Chen, L., Xiong, J., Chen, X., Lee, S.I., Zhang, D., Yan, T. and Fang, D.: LungTrack: Towards Contactless and Zero Dead-Zone Respiration Monitoring with Commodity RFIDs, *Proc. ACM Interact. Mob. Wearable Ubiquitous Technol.*, Vol.3, No.3 (online), DOI: 10.1145/3351237 (2019).

[78] Liu, C., Xiong, J., Cai, L., Feng, L., Chen, X. and Fang, D.: Beyond Respiration: Contactless Sleep Sound-Activity Recognition Using RF Signals, *Proc. ACM Interact. Mob. Wearable Ubiquitous Technol.*, Vol.3, No.3 (online), DOI: 10.1145/3351254 (2019).

[79] Xu, H., Wang, D., Zhao, R. and Zhang, Q.: AdaRF: Adaptive RFID-Based Indoor Localization Using Deep Learning Enhanced Holography, *Proc. ACM Interact. Mob. Wearable Ubiquitous Technol.*, Vol.3, No.3 (online), DOI: 10.1145/3351271 (2019).

[80] Huang, A., Wang, D., Zhao, R. and Zhang, Q.: Au-Id: Automatic User Identification and Authentication through the Motions Captured from Sequential Human Activities Using RFID, *Proc. ACM Interact. Mob. Wearable Ubiquitous Technol.*, Vol.3, No.2 (online), DOI: 10.1145/3328919 (2019).

[81] Wang, Y. and Zheng, Y.: Modeling RFID Signal Reflection for Contact-Free Activity Recognition, *Proc. ACM Interact. Mob. Wearable Ubiquitous Technol.*, Vol.2, No.4 (online), DOI: 10.1145/3287071 (2018).

[82] Wang, C., Xie, L., Wang, W., Chen, Y., Bu, Y. and Lu, S.: RF-ECG: Heart Rate Variability Assessment Based on COTS RFID Tag Array, *Proc. ACM Interact. Mob. Wearable Ubiquitous Technol.*, Vol.2, No.2 (online), DOI: 10.1145/3214288 (2018).

[83] Chang, L., Xiong, J., Wang, J., Chen, X., Wang, Y., Tang, Z. and Fang, D.: RF-Copybook: A Millimeter Level Calligraphy Copybook Based on Commodity RFID, *Proc. ACM Interact. Mob. Wearable Ubiquitous Technol.*, Vol.1, No.4 (online), DOI: 10.1145/3161191 (2018).

[84] Jin, H., Yang, Z., Kumar, S. and Hong, J.I.: Towards Wearable Everyday Body-Frame Tracking Using Passive RFIDs, *Proc. ACM Interact. Mob. Wearable Ubiquitous Technol.*, Vol.1, No.4 (online), DOI: 10.1145/3161199 (2018).

[85] Wang, J., Chang, L., Aggarwal, S., Abari, O. and Keshav, S.: Soil Moisture Sensing with Commodity RFID Systems, *Proc. 18th International Conference on Mobile Systems, Applications, and Services, MobiSys '20*, pp.273–285 (online), DOI: 10.1145/3386901.3388940 (2020).

[86] Wikipedia: The Thing (listening device), Wikipedia (online), available from ⟨https://en.wikipedia.org/wiki/The_Thing_(listening_device)⟩ (accessed 2020-10-05).

[87] Wikipedia: Laser microphone, Wikipedia (online), available from ⟨https://en.wikipedia.org/wiki/Laser_microphone⟩ (accessed 2020-10-05).

[88] Iyer, V., Chan, J. and Gollakota, S.: 3D Printing Wireless Connected Objects, *ACM Trans. Graph.*, Vol.36, No.6 (online), DOI: 10.1145/3130800.3130822 (2017).

[89] Gao, C., Li, Y. and Zhang, X.: LiveTag: Sensing Human-Object Interaction through Passive Chipless WiFi Tags, *15th USENIX Symposium on Networked Systems Design and Implementation* (*NSDI '18*), pp.533–546 (online), available from ⟨https://www.usenix.org/conference/nsdi18/presentation/gao⟩ (2018).

[90] Ryoo, J., Karimi, Y., Athalye, A., Stanaćević, M., Das, S.R. and Djurić, P.: BARNET: Towards Activity Recognition Using Passive Backscattering Tag-to-Tag Network, *Proc. 16th Annual International Conference on Mobile Systems, Applications, and Services, MobiSys '18*, pp.414–427 (online), DOI: 10.1145/3210240.3210336 (2018).

[91] Ranganathan, V., Gupta, S., Lester, J., Smith, J.R. and Tan, D.: RF Bandaid: A Fully-Analog and Passive Wireless Interface for Wearable Sensors, *Proc. ACM Interact. Mob. Wearable Ubiquitous Technol.*, Vol.2, No.2 (online), DOI: 10.1145/3214282 (2018).

[92] Waghmare, A., Xue, Q., Zhang, D., Zhao, Y., Mittal, S., Arora, N., Byrne, C., Starner, T. and Abowd, G.D.: UbiquiTouch: Self Sustaining Ubiquitous Touch Interfaces, *Proc. ACM Interact. Mob. Wearable Ubiquitous Technol.*, Vol.4, No.1 (online), DOI: 10.1145/3380989 (2020).

[93] Tong, X., Zhu, F., Wan, Y., Tian, X. and Wang, X.: Batch Localization Based on OFDMA Backscatter, *Proc. ACM Interact. Mob. Wearable Ubiquitous Technol.*, Vol.3, No.1 (online), DOI: 10.1145/3314412 (2019).

Akira Uchiyama received his M.E. and Ph.D. degrees in Information and Computer Science from the Osaka University in 2005 and 2008, respectively. He is an Assistant Professor at Graduate School of Information Science and Technology, Osaka University. He was a visiting scholar in the University of Illinois at Urbana-Champaign in 2008 and a research fellow of the Japan Society for the Promotion of Science from 2007 to 2009. His current research interests include mobile sensing and applications in pervasive and ubiquitous computing. He is a member of IEEE, ACM, IEICE and IPSJ.

Shusuke Saruwatari received his Dr. Sci. degree from the University of Tokyo in 2007. From 2007 to 2008, he was a visiting researcher at the Illinois Genetic Algorithm Laboratory, University of Illinois at Urbana-Champaign. From 2008 to 2012, he was a research associate at the RCAST, the University of Tokyo. From 2012 to 2016, he was an assistant professor at Shizuoka University. He has been an associate professor at Osaka University Since 2016. His research interests are in the areas of wireless networks, sensor networks, and system software.

Takuya Maekawa is an Associate Professor in the Graduate School of Information Science and Technology, Osaka University. He received his bachelor degree from School of Engineering, Osaka University in 2003. In 2004, he received his master degree from Graduate School of Information Science and Technology, Osaka University. In 2006, he received his doctor degree (Information Science and Technology) from Graduate School of Information Science and Technology, Osaka University. After that he worked for NTT Communication Science Laboratory for six years. He was awarded the IPSJ/IEEE Computer Society Young Computer Researcher Award on the topic of zero-shot and few-shot unobtrusive context recognition for pervasive computing in 2019. His research interest includes sensor-based context recognition techniques for pervasive/ubiquitous computing.

Kazuya Ohara is a Researcher at NTT Communication Science Laboratories in Kyoto, Japan. He received his B.E. degrees, the Master of information science and technology degrees, and his Ph.D. in information science and technology from Osaka University in 2015, 2016, and 2019, respectively. He joined NTT Communication Science Laboratories in 2019. His research interests include ubiquitous computing and machine learning. He is a member of IEEE and IPSJ.

Teruo Higashino received his B.S., M.S. and Ph.D. degrees in Information and Computer Sciences from Osaka University, Japan in 1979, 1981 and 1984, respectively. He joined the faculty of Osaka University in 1984. Since 2002, he has been a Professor in Graduate School of Information Science and Technology at Osaka University. His current research interests include design and analysis of distributed systems, communication protocol and mobile computing. He is a senior member of IEEE, a fellow of Information Processing Society of Japan (IPSJ), and a member of ACM and IEICE of Japan.